ZP2 peptide beads select human sperm in vitro, decoy mouse sperm in vivo, and provide reversible contraception

Matteo A. Avella[1], **Boris A. Baibakov**[1], **Maria Jimenez-Movilla**[2], **Anna Burkart Sadusky**[1], and **Jurrien Dean**[1,*]

[1]Laboratory of Cellular and Developmental Biology, National Institute of Diabetes and Digestive and Kidney Diseases, National Institutes of Health, Bethesda, MD 20892, USA.

[2]Department of Cell Biology and Histology, Medical School, University of Murcia, IMIB, 30100 Murcia, Spain.

Abstract

Gamete recognition in the female reproductive tract occurs at the surface of the zona pellucida surrounding ovulated eggs. The acellular zona matrix is composed of three (mouse) or four (human) proteins (ZP1 to ZP4), and the amino terminus of ZP2 is the primary sperm-binding ligand. Mouse and human sperm bind, respectively, to recombinant $moZP2^{35-149}$ and $huZP2^{39-154}$ peptides attached to agarose beads. Mouse ZP2 peptide beads markedly inhibited fertilization of ovulated mouse eggs inseminated in vitro and incubated overnight. Similarly, human ZP2 peptide beads prevented sperm binding and penetration of transgenic *ZP2^Rescue* zonae pellucidae, in which human ZP2 replaced mouse ZP2. When mouse ZP2 peptide beads were transcervically deposited into the uterus, there was no change in mating behavior and copulatory plugs were present, but bound sperm did not progress into the oviduct and female mice were infertile. On average, contraception lasted >10 estrus cycles but was reversible with no detectable pathology in the reproductive tract. Despite the long-term contraceptive effect, initial sperm binding to the peptide beads was reversible in vitro. We exploited this observation to select human sperm that were better able to penetrate the zonae of human *ZP2^Rescue* eggs, and the approach holds promise for identifying superior sperm for human assisted reproductive technologies (ART). We conclude that the amino-terminal ZP2 peptide supports sperm binding, which is initially reversible but, with time, becomes irreversible. Short-term, reversible binding may be useful in selecting sperm for ART, and long-term binding decoys sperm and results in effective contraception in mice.

INTRODUCTION

Improved reproductive choice requires more robust options for contraception as well as enhanced assisted reproductive technologies (ART) for treatment of infertility. The current world population (7.2 billion) is expected to increase to 9.6 billion to 12.3 billion by 2100 (1), giving immediacy to the discovery of innovative and effective contraceptive strategies. Conversely, improved gamete selection would materially benefit successful outcomes for ART in the treatment of infertility that affects roughly one in eight couples (2). A compelling target for nonhormonal modulation of fertility is the zona pellucida, an extracellular matrix surrounding ovulated eggs and the preimplantation embryo. The zona pellucida is composed of three (mouse) or four (human) homologous glycoproteins designated as ZP1 to ZP4 (3, 4).

Successful mammalian fertilization requires sperm binding to ZP2. Human sperm do not bind to the mouse zona pellucida (5) but will bind and penetrate genetically engineered mouse zona pellucida, in which human ZP2 replaces the endogenous mouse protein (hu$ZP2^{Rescue}$ mice). The penetrating human sperm do not bind or fuse with mouse eggs but accumulate in the perivitelline space between the zona matrix and the plasma membrane (6). After fertilization, egg cortical granules release ovastacin (7), a zinc metalloendoprotease that cleaves the N terminus of ZP2 to prevent gamete recognition and polyspermy (8, 9). Recent progress in understanding the molecular basis of gamete recognition has documented that the N terminus of ZP2 is necessary and sufficient for human and mouse sperm binding and essential for female mouse fertility. Recombinant mouse and human ZP2 N-terminal peptides (moZP2$^{35–149}$ or huZP2$^{39–154}$) produced in baculovirus and attached to agarose beads can support in vitro binding of their cognate sperm (10).

Our current studies investigate the ability of the N terminus of ZP2 to (i) select human sperm better able to bind and penetrate the zona pellucida and (ii) decoy sperm in the female reproductive tract for reversible contraception. Existing selection criteria for sperm used in ART are based on Kruger's strict morphology (11), sperm motility, and the ability of sperm to bind hyaluronic acid and penetrate through the cumulus oophorus or bind in a hemizona assay. However, none seem ideal (12). We now report that human sperm isolated by ZP2 peptide beads show enhanced ability to bind and penetrate zonae pellucidae surrounding ovulated hu$ZP2^{Rescue}$ eggs. In addition, we document the ability of N-terminal ZP2 peptides attached to agarose beads to decoy mouse sperm and prevent fertilization in vitro. After intrauterine administration, sperm bound to the ZP2 peptide beads and did not progress into the oviduct to encounter ovulated eggs, which provided long-term, reversible contraception in vivo.

RESULTS

Acr^{mCherry} sperm bind to ZP2 peptide beads

A transgene (Fig. 1A) in which complementary DNA (cDNA) encoding mCherry replaced enhanced green fluorescent protein (EGFP) in Acr^{EGFP} (13) was used to establish mouse lines (fig. S1A). Under the control of the acrosin promoter, these mice expressed fluorescent mCherry that accumulated in the acrosomes overlying the anteriorly located sperm nucleus

and was detected before, but not after, induction of acrosome exocytosis (Fig. 1B). The $Acr^{mCherry}$ transgenic mice were fertile with normal litter sizes. Their sperm had normal morphology and motility as determined by computer-assisted sperm analysis (CASA-IVOS) (fig. S1B).

To test whether sperm, immediately after release from the epididymis, have the ability to bind the zona pellucida or the N terminus of ZP2, we isolated $Acr^{mCherry}$ and Acr^{EGFP} (13) sperm from epididymides into the human tubal fluid (HTF) medium supplemented with bovine serum albumin (BSA) and used immediately or after a 1-hour incubation at 37°C, respectively. After either treatment, fluorescently tagged sperm bound within 5 min to the zona pellucida surrounding cumulus-free eggs either alone or as a 1:1 mixture (Fig. 1C and fig. S1C). Mouse sperm also bound to moZP2$^{35-149}$ peptide beads (Fig. 1, D and E, and fig. S1D), but not to beads alone (fig. S1E), and previous incubation (1 hour) in HTF/BSA medium did not affect the number of sperm that initially bound (Fig. 1F). We conclude that mouse and human sperm incubated for as little as 5 min in HTF/BSA can bind to the N terminus of ZP2 in numbers comparable to those observed at 1 hour. This is consistent with reports that sperm bind in vitro to the zona pellucida surrounding eggs before capacitation (14), which is required for acrosome exocytosis and fertilization (15, 16).

MoZP2$^{35-149}$ peptide beads inhibit in vitro fertilization

To determine whether moZP2$^{35-149}$ could decoy sperm, we inseminated eggs in cumulus mass in vitro with 1×10^5 sperm in 500 µl of medium in the presence of moZP2$^{35-149}$ peptide beads (3000 beads/µl) or agarose beads (3000 beads/µl) lacking zona peptides (Fig. 2A). In the absence of beads or in the presence of beads alone, 84.5 ± 1.6% [average (avg) ± SEM] and 75.8 ± 1.6% of eggs were fertilized, respectively. However, in the presence of moZP2$^{35-149}$ peptide beads, only 6.8 ± 3.8% of the eggs were fertilized after a 24-hour incubation (Fig. 2B).

MoZP2$^{35-149}$ peptides incubated for 1 hour with live epididymal sperm bound to the anterior surface and postacrosomal region of acrosome-intact sperm and trans-located to the equatorial segment after spontaneous acrosome exocytosis (Fig. 2C). Under identical experimental conditions, reduced and alkylated moZP2 peptides lacking secondary structure did not bind at all to acrosome-intact or acrosome-reacted sperm (fig. S2, A and B). To study the effect of sperm–peptide bead interactions in vitro, we added 10 ml of moZP2$^{35-149}$ peptide beads (300 beads/µl) to 1×10^5 progressive motile $Acr^{mCherry}$ sperm immediately after or 1 hour after release from the epididymis in 500 µl of HTF/BSA. At 5 min to 8 hours after insemination, we determined the number, motility, and acrosome status of bound sperm, as well as the motility of the free sperm in the medium. Sperm freshly released from the epididymis or incubated in medium for 1 hour before insemination bound to the peptide beads in comparable numbers (fig. S2, C and D). Unbound sperm in the medium maintained progressive motility for 2 hours after insemination but completely lost their motility by 4 hours (Fig. 2D), at which time the beads to which sperm were bound no longer rotated (fig. S2E).

Both freshly released sperm from the epididymis and sperm that were incubated for 1 hour in medium before insemination, which then bound to the ZP2 peptide beads, underwent

acrosome exocytosis between 60 min and 4 hours after insemination (Fig. 2E), but acrosome-reacted, nonmotile sperm remained bound to the peptide bead as determined by light (fig. S2, C and D) and electron microscopy (Fig. 2F), presumably via the equatorial region to which the moZP2$^{35-149}$ peptide remained bound (Fig. 2C, right panel). We conclude that over time, sperm decoyed by the moZP2 peptide beads lose motility, lose membrane integrity, and are unable to fertilize eggs.

HuZP2$^{39-154}$ peptide beads inhibit zona matrix penetration by human sperm

To extend these observations to human biology, we documented that human sperm, either freshly thawed or incubated in HTF/BSA for 2 hours before insemination, bound to huZP2$^{39-154}$ peptide beads (Fig. 1, D and F, and fig. S3, A and B). Sperm binding and zona penetration were assayed using hu*ZP2^Rescue* eggs from transgenic mice, in which huZP2 replaced endogenous moZP2 (6). Hu*ZP2^Rescue* eggs in cumulus and 1×10^5 progressive motile human sperm were incubated overnight in medium (500 ml), beads alone (3000 beads/μl), or huZP2$^{39-154}$ peptide beads (3000 beads/μl) (Fig. 3A). Progressive motility of unbound sperm was maintained for at least 2 hours (Fig. 3B). In the presence of medium, beads alone, or moZP2$^{35-149}$ peptide beads, one to five human sperm were observed in the perivitelline space of these eggs. However, in the presence of huZP2$^{39-154}$ peptide beads, no sperm were present in the perivitelline space of 27 hu*ZP2^Rescue* eggs, and a single human sperm was observed in the 28th egg (Fig. 3C). We conclude that moZP2$^{35-149}$ and huZP2$^{39-154}$ peptide beads are effective in decoying mouse and human sperm, respectively, and preventing them from binding and penetrating the zona pellucida surrounding ovulated eggs in cumulus, even when the number of sperm is substantially greater than encountered in vivo (17).

HuZP2$^{39-154}$ peptide beads select sperm competent for binding and penetration of the zona pellucida

In the peptide bead–binding experiments, we observed that 30 min after insemination, human sperm bound to the beads were loose and easily detached by gentle pipetting. To determine whether the initially bound sperm have a superior ability to penetrate the zona matrix, we incubated 1×10^5 progressive motile human sperm in 500 μl of medium with beads alone (300 beads/μl) or huZP2 peptide beads (300 beads/μl) for 30 min and transferred to a second dish where sperm and beads were separated by gentle pipetting (fig. S3C). Beads were then removed under microscopic visualization. The remaining sperm, selected for their ability to reversibly bind to the huZP2 peptide beads, were fixed and immunostained with antibodies to sperm equatorial segment protein 1 (SPESP1) and CD46 (6) to determine whether the acrosome was intact or reacted, respectively. Under these experimental conditions, $62.6 \pm 10.4\%$ (avg ± SEM) of the human sperm were acrosome-intact compared to the starting population in which $53.2 \pm 5.2\%$ sperm were acrosome-intact.

To investigate the biological activity of the selected sperm from individual donors, we added 5 to 10 hu*ZP2^Rescue* eggs in cumulus mass after the removal of the beads under microscopic visualization (fig. S3C). Using sperm (~10^3 ml^{-1}) from five anonymous, fertile human donors, the number of sperm that bound to the surface of the zona pellucida (Fig. 4, A to C, and fig. S4, A and B) or penetrated through the zona matrix (Fig. 4, D to F, and fig. S4, C

and D) was substantially increased after selection with huZP2 peptide beads compared to unselected sperm incubated with medium or beads alone. The five donors differed in the number of sperm bound to the zona pellucida [donor A, 2.0 ± 0.5 (avg $\pm$ SEM); donor B, 8.6 ± 2.2; donor C, 4.8 ± 0.6; donor D, 4.2 ± 0.9; donor E, 4.3 ± 0.7) and in the number of sperm in the perivitelline space (donor A, 2.0 ± 0.5; donor B, 2.2 ± 0.7; donor C, 6.1 ± 1.1; donor D, 3.7 ± 0.7; donor E, 2.7 ± 0.4) (fig. S4).

To document that the selected human sperm could bind to native human zonae pellucidae, we removed the beads and added four to seven immature human zonae pellucidae (Fig. 4G). After 1 hour of incubation, human sperm bound robustly to the native zona matrix and were quantified after fixation and confocal microscopy (avg $\pm$ SEM; donor A, 55.2 ± 7.8 sperm per zona; donor B, 43.5 ± 4.4 sperm per zona; donor C, 105.6 ± 15.0 sperm per zona), with results that were comparable to earlier reports (18, 19). From these observations, we conclude that human sperm selection with huZP2 peptide beads is a rapid (35 min) and effective procedure to identify subpopulations of sperm competent for zona pellucida binding and penetration. These results suggest utility in the clinic to improve the outcome of ART for humans.

MoZP2$^{35-149}$ peptide beads act to decoy sperm in vivo

To determine whether the same sperm decoy effect observed in vitro could be achieved in vivo, we transcervically administered moZP2$^{35-149}$ peptide beads or beads alone (1.5×10^6) (Fig. 5A) into the bilateral uterine horns of mice using a 1-ml syringe attached to a blunted plastic needle (10). To assay the effectiveness of this procedure, we confirmed the presence of moZP2$^{35-149}$ peptide on the moZP2 peptide beads in vitro with a monoclonal antibody to ZP2$^{N\text{-term}}$ (Fig. 5B). After intrauterine administration, the reproductive tract was fixed and clarified for 3 weeks with Sca*l*eA2 (20), and ZP2 peptide beads were detected throughout the uterus by confocal microscopy. No immuno-reactivity with the anti-ZP2 antibody was observed after administration of beads alone, which were identified by staining with wheat germ agglutinin (Fig. 5C).

We hypothesized that precocious interaction between sperm and moZP2 peptide beads would impede sperm progression after intrauterine ejaculation and cause infertility. To follow sperm migration and acrosome status, we crossed $Acr^{mCherry}$ mice with $Prm1^{EGFP}$ (21) and $Figla^{EGFP}$ (22) mice to establish $Acr^{mCherry}$; $Prm1^{EGFP}$; $Figla^{EGFP}$ mice in which protamine^{EGFP} was present in the nucleus, myristoylated EGFP was embedded in the plasma membrane, and mCherry was present in the acrosome. These mice were fertile with normal litter sizes, and their sperm had normal morphology, albeit with a decrease in the number of sperm with progressive motility as determined by CASA-IVOS (Fig. 5D and fig. S1B).

Eggs in cumulus oophorus from $Zp3^{EGFP}$ female mice with a green zona pellucida (23) were inseminated in vitro with $Acr^{mCherry}$; $Prm1^{EGFP}$; $Figla^{EGFP}$ sperm. After 5 min, sperm and eggs were fixed and clarified and then imaged by confocal microscopy, where both acrosome-intact (yellow heads) and acrosome-reacted sperm (green heads) could be observed at single-cell resolution (Fig. 5E). These fixation and clarification procedures were used to determine whether sperm competent for binding and zona matrix penetration reach the oviductal ampulla after encountering the moZP2 peptide beads in the uterus. To avoid

possible inconsistencies with in vivo fertilization (time of insemination, dissolution of the cumulus oophorus, etc.), we crossed $Zp3^{EGFP}$ mice into the $Cd9$ (24) null background to inhibit gamete fusion (and fertilization), which allowed sperm to accumulate in the perivitelline space. Female mice were treated with HTF medium, beads alone, or moZP2 peptide beads before overnight mating with $Acr^{mCherry}$; $Prm1^{EGFP}$; $Figla^{EGFP}$ male mice. Female mice with copulatory plugs were anesthetized 14 hours after mating and perfused by transcardiac administration of phosphate-buffered saline (PBS)/heparin. After fixation and clarification of the female reproductive tract, acrosome-reacted and acrosome-intact sperm bound to moZP2 peptide beads were detected in the uterus at single-cell resolution, but no sperm were observed in the oviduct (Fig. 5F). In contrast, sperm were present in the oviduct of female mice treated with medium (fig. S5A) or beads alone (Fig. 5F), and $Zp3^{EGFP}$; $Cd9^{Null}$ eggs accumulated sperm in their perivitelline space. The nonfertilizing sperm in the ampulla of the oviduct were acrosome-reacted (green in Fig. 5F, lower panel), whereas those in the uterus and lower oviduct were mostly acrosome-intact (yellow in Fig. 5F, upper panel flyout), consistent with previous observations (25, 26).

MoZP2$^{35-149}$ peptide beads provide long-term reversible contraception in female mice

The four cysteine residues in moZP2$^{35-149}$ that form two disulfide bonds were reduced and alkylated (fig. S5B) to confirm the specificity of the mouse peptide as a sperm decoy. Sperm bound robustly to the native moZP2$^{35-149}$ peptide beads (26.3 ± 0.2 sperm, avg ± SEM), but little, if at all (1.3 ± 0.3), after the peptide had been reduced and alkylated (fig. S5, C and D). Consequently, the reduced and alkylated moZP2$^{35-149}$ peptide beads had little inhibitory effect on in vitro (fig. S5E) or in vivo (fig. S5F) fertilization, and beads alone were used as negative controls in subsequent experiments.

Gonadotrophin-stimulated normal female mice were mated with fertile males after treatment with medium, beads alone, or moZP2$^{35-149}$ peptide beads (~1.5 × 10^6 beads in 500 μl). Embryos from females with copulatory plugs were isolated 48 hours after mating. Females ($n = 5$) treated with medium or beads alone were fertile, and 21.0 ± 2.1 (avg ± SEM) and 17.7 ± 1.2 two-cell embryos, respectively, were recovered from their oviducts 40 hours after mating. Embryos were rarely (1.3 ± 0.3) observed in females (n = 5) treated with moZP2 peptide beads (Fig. 6A).

To investigate an effect on the female mice ($n = 5$) treated with medium, beads alone, or moZP2 peptide beads, the female mice were co-caged and continuously mated with a male proven to be fertile (1:3). Female mice treated with beads alone or medium became pregnant and delivered pups 25.4 ± 0.6 (avg ± SEM) and 28.2 ± 3.1 days after mating, respectively. Female mice treated with moZP2 peptide beads were initially infertile and did not give birth to pups until 72.8 ± 4.6 days after mating. The first moZP2 peptide bead–treated litters were smaller (3.2 ± 1.2 versus 7.2 ± 1.5) (avg ± SEM) than the beads alone control, but matched them (8.0 ± 0.7 versus 8.4 ± 1.5) by the second litter. All of the moZP2 peptide bead–treated mice eventually resumed fertility and produced at least two litters within the 5-month study (Fig. 6B), by the end of which no beads were present in the uterine cavity. To investigate potential pathology as causative of the observed infertility, we isolated the reproductive tracts of female mice 14 days after treatment. Compared to female mice treated with beads

alone, no histopathology or evidence of inflammation was observed in female mice treated with moZP2 peptide beads (Fig. 6C). Thus, we conclude that moZP2 peptide bead treatment results in long-term, reversible contraception with no obvious adverse effects.

DISCUSSION

Effective contraception is critical for family planning and includes barrier methods, hormone intervention, intrauterine devices, and sterilization (27). Newer methods for male contraception reversibly prevent sperm maturation (28, 29), disrupt the Sertoli cell barrier to promote sperm loss (30, 31), or affect sperm motility (30). As an alternative approach, we now provide evidence that decoying sperm in the lower female reproductive tract with ZP2 N-terminal peptide beads prevents interactions with ovulated eggs. This strategy provides highly effective, nonhormonal, long-term, but reversible contraception in female mice. The N terminus of huZP2 has a comparable effect on human sperm in vitro, and ZP2 is conserved among eutherian mammals (32). Thus, we envision that the sperm-decoy strategy can be translated to theriogenology and reproductive medicine to provide effective female contraception.

Normally, sperm undergo capacitation during passage through the female reproductive tract or after incubation with serum proteins to gain the ability to fertilize ovulated eggs (15, 16). Neither mouse nor human sperm need to be incubated in HTF/BSA medium longer than 5 min to bind to the peptide beads, which provide immediate capture of sperm after initial contact with the ZP2 N-terminal peptide both in vitro and in vivo. After 4 (mouse) to 8 (human) hours, bound sperm lose their motility as well as the integrity of the plasma and outer acrosome membranes in vitro and remain adherent to the beads. Once irreversibly bound to the peptide beads, sperm do not ascend through the uterotubal junction and are not observed in the oviduct. Whether all sperm interact with the peptide beads or just a sufficient number to fall below a threshold needed to progress into the upper female reproductive tract remains to be determined. It appears that inert beads (37- to 100-μm diameter) themselves are no obstacle to sperm passage through the uterus, because female mice treated with beads alone had normal in vitro and in vivo fertility. In these proof-of-principle experiments, the peptide beads provided effective, long-term contraception that was ultimately reversible. To better provide contraception on demand, it may be beneficial to combine the ZP2 peptide beads with spermicidal gels or attach them to removable spermicidal sponges. Alternatively, the ZP2 peptides could be attached to vaginal rings impregnated with steroid hormones (estrogen and progestin) to improve contraceptive efficacy by decreasing available sperm and suppressing ovulation.

Sperm binding to the N terminus of ZP2 in vitro may also provide a physiological criterion to identify sperm for ART. Intracytoplasmic sperm injection, in which a single human spermatozoon is injected directly into a retrieved egg (33), relies on anthropomorphic selection of one sperm out of many, and successful outcome may not be apparent until birth or later in life (34). We used huZP2 peptide beads to select human sperm that have an improved ability to bind and penetrate the hu*ZP2^Rescue* zona pellucida and bind robustly to native human zona pellucida. The advantage of sperm selection with huZP2 peptide beads is multifold. The recombinant human peptide provides an inexhaustible supply of reagents, and

commercial production of the peptide beads is technologically simple. The selection procedure takes ~30 min and can be supplemented by secondary criteria such as sperm morphology and/or motility. It may be useful to concentrate sperm in patients with oligozoospermia (<20 million sperm ml^{-1}), select better performing sperm from patients with asthenozoospermia (<50% normal motility or <25% any motility), and discriminate between normal and abnormal sperm in patients with teratozoospermia (<30% normal morphology).

Although the findings are promising, further validation of these observations is required. Double-blind clinical trials will be needed to determine the relative merit of choosing sperm with huZP2 peptide beads compared to existing selection procedures. It remains to be seen whether selected sperm will result in better outcomes for in vitro fertilization or intracytoplasmic sperm injections, and it is not yet clear how that will be determined and whether it will be consistent across mammalian species. Despite its effectiveness in a rodent model, the ability of ZP2 peptide beads to decoy sperm in the female reproductive tract needs to be assessed in more translationally relevant mammals. Similarly, agarose beads may not be the optimal substrate to tether the ZP2 peptides for delivery into the female reproductive tract, and alternatives will need to be explored. In addition, the long-term effects of repeated administration of ZP2 peptides are unknown and remain a concern given the association of autoimmune oophoritis with zona pellucida–based contraceptive vaccines (35).

Last, we used perfusion and clarification strategies developed for brain tissue (20) to image fluorescently tagged sperm (*Acr^{mCherry}*; *Prm1^{EGFP}*;*Figla^{EGFP}*) and determine their localization and acrosome status with single-cell resolution. Coupled with the use of fluorescently tagged eggs (for example, *Zp3^{EGFP}*), these approaches may be proven useful for investigations in oocyte maturation within the ovary, the acrosome status of sperm as they traverse the female reproductive tract, fertilization within the cumulus oophorus in the ampulla of the oviduct, and embryonic progression during preimplantation development.

MATERIALS AND METHODS

Study design

These investigations are based on the recent observation in transgenic mice that sperm bind to the N terminus of ZP2 in the extracellular zona pellucida surrounding mouse and human eggs. The objectives of the current studies were twofold. The first objective was to determine whether mouse N-terminal ZP2 peptides attached to agarose beads could act as a decoy to bind mouse sperm and prevent in vitro fertilization. These studies were then extended by transcervical administration of control beads and peptide beads, which resulted in long-term, reversible contraception in vivo. The second objective was to translate these observations from mouse to human by using huZP2 peptide beads to prevent human sperm from penetrating zonae pellucidae, in which huZP2 replaces moZP2. The success of this approach prompted further investigations into using the huZP2 peptide beads to select superior sperm for ART, as judged by their ability to bind and penetrate huZP2 rescue zonae pellucidae better than unselected sperm. The results were confirmed by using multiple, randomly selected, anonymous, fertile sperm donors to minimize bias. These studies also introduced

the use of Sca*l*eA2 to clarify the female reproductive tract and facilitate observations of fluorescently tagged sperm and eggs in fixed tissues.

Establishment of mouse lines with fluorescent sperm

DNA encoding EGFP was released from *Acr3*^{EGFP} (13) in pUC19 by digestion with Pst I (New England Biolabs) and treated with Klenow (Promega) to generate blunt ends. We used mCherry (Takara Clontech) as a template to synthesize mCherry + SV40 poly(A) cDNA by polymerase chain reaction (PCR) with oligonucleotides flanking the Eco RV restriction sites (forward, 5′-GATATCACCATGGTGAGCAAGGGC-3′; reverse, 5′-GATATCCACCATGGTGAGCAAGGGC-3′). The PCR product was subcloned into pCR2.1, isolated after digestion with Eco RV, and blunt end–ligated into pUC19-Acr3 to establish a transgene with an acrosin promoter (2.4 kb), the proacrosin signal peptide (MVEMLPTVAVLVLAVSVVA) including an N-terminal peptide (KDNTT) in-frame with the mCherry cassette, analogous to *Acr3*^{EGFP}.

The transgene was isolated with Bam HI and Hind III (New England Biolabs), gel-purified, and injected into the male pronucleus of fertilized FVB/N eggs. Mice were genotyped by PCR (95°C for 30 s, 58°C for 30 s, 72°C for 1 min ×30 cycles, 72°C for 7 min, and 4°C for >30 min) using mouse tail DNA and primers that amplified a 507–base pair region across the 5′ untranslated region of Acrosin and mCherry (forward, 5′-TTTGTGAGGTCACAGCTTGC-3′; reverse, 5′-GTAGATGAACTCGCCGTCCT-3′). Expression of the *Acr*^{mCherry} transgene was detected by reverse transcription PCR with a gene-specific primer set (table S1) and total RNA isolated from a 12-week-old male mouse tissue (fig. S1A). *Gapdh* transcripts served as a control for RNA integrity (table S1) (10).

Three founder males passed the transgene through their germ line and accumulated mCherry in their acrosomes. One line, Tg(Acr/mCherry1Dean), was used in the experiments reported and designated as *Acr*^{mCherry}. This line was crossed with the *Prm1*^{EGFP} (21) and the *Figla*^{EGFP} (with myristoylated EGFP embedded in the plasma membrane) (22) lines to obtain a mouse line with sperm that accumulates mCherry in the acrosome and EGFP in the sperm nucleus and in the plasma membrane (*Acr*^{mCherry}; *Prm1*^{EGFP}; *Figla*^{EGFP}).

All mice were handled in compliance with the guidelines of the Animal Care and Use Committee of the National Institutes of Health under the Division of Intramural Research, National Institute of Diabetes and Digestive and Kidney Diseases (NIDDK), which approved the animal study protocols.

Preparation of mouse and human gametes

Normal or transgenic mouse sperm were released from cauda epididymides in HTF (EMD Millipore) supplemented with 0.4% BSA (Sigma-Aldrich) and analyzed by CASA-IVOS (10). Mouse sperm were incubated for 1 hour (37°C, 90% N_2, 5% O_2, 5% CO_2) to ensure capacitation before use. Control (ICR) or *Zp3*^{EGFP} (23) female mice were stimulated with 5 IU of equine chorionic gonadotropin (eCG) and human chorionic gonadotropin (hCG) (Sigma-Aldrich), and eggs in cumulus were collected 12 hours after hCG injection and incubated as described above in 500 μl of HTF with 0.4% BSA at a final concentration of 1 × 10^5 ml^{-1} progressive motile sperm (9, 10). Fertilization was scored 24 hours later by the

presence of two-cell embryos. To assess in vivo fertility, males (5) from each mouse line were singly co-caged with control fertile female mice, and litters were recorded until females gave birth to at least two litters.

To isolate human sperm, human semen (Genetics & IVF Institute Cryobank) was added to an Eppendorf tube (2.0 ml) containing 0.5 ml of 40% of PureSperm (Nidacon) layered over 0.5 ml of 80% PureSperm (http://nidacon.com/ifu/density_gradient.pdf). After centrifugation (swinging bucket, 20 min × 300g) and removal of the supernatant, the sperm pellet was resuspended in the residual buffer and transferred into 1.0 ml of HTF. After a second centrifugation (5 min × 300g), sperm were resuspended in 0.2 ml of HTF/BSA and diluted in 500 μl of HTF with 0.5% BSA to 1×10^5 ml^{-1} progressive motile sperm (6, 36). Human sperm were incubated (37°C, 90% N_2, 5% O_2, 5% CO_2) in HTF/BSA for 4 hours (10).

Light microscopy

Fixed gamete samples (1 hour, 2 to 4% paraformaldehyde) were mounted in PBS, and images of eggs, embryos, and beads were obtained with an LSM 780 confocal microscope (Carl Zeiss AG) using a 63×/1.2 NA (numerical aperture) water immersion objective lens at room temperature (10). Images were exported as full resolution TIF files and processed in Photoshop CS6 (Adobe Systems) to adjust brightness and contrast. Alternatively, confocal optical sections were projected on a single plane with maximum intensity and combined with DIC images of sperm, eggs, or peptide beads using LSM image software.

For live imaging of acrosome exocytosis, $Acr^{mCherry}$ sperm were incubated with A23187 (6). To examine sperm peptide bead interactions, moZP2$^{35-149}$ peptide beads (300 beads/ml) were inseminated with 10^5 progressive motile $Acr^{mCherry}$ mouse sperm. Z sections were collected every 15 s by confocal microscopy for 8 hours after insemination using a 20×/0.8 NA objective lens and a 35-mm glass-bottom, 14-mm microwell dish (MatTek) incubated (37°C, 90% N_2, 5% O_2, 5% CO_2) in a Gas Incubation System (ibidi) (10). Projections of confocal and DIC images were obtained and analyzed by ZEN and LSM software. The centers of each bead/circle were tracked at each time point with individual dots, which were connected with straight lines to summarize the beads' translocation over time.

To analyze moZP2 peptide bead binding to sperm, $Acr^{mCherry}$ sperm were released from the isolated epididymides in 100 μl of 0.4% HTF/BSA. After a 1-hour incubation (37°C, 5% CO_2), sperm (1×10^6 progressive motile) were added to 2.0 ml of pre-equilibrated moZP2$^{35-149}$ peptide (PBS, 1.5 mg/ml) for an additional hour under the same conditions. A 2% formaldehyde solution (Invitrogen) was used to cross-link sperm and peptide (30 min, 20°C, end-over-end rotation). After centrifugation (5 min, 4000g), the sperm were resuspended (1.0 ml of PBS/BSA), fixed (3.7% formaldehyde, 5 min, 20°C), resuspended in blocking solution (1.0 ml of PBS, 0.1% Tween 20, 0.5% BSA), and incubated (overnight, 4°C) with a monoclonal antibody (1:50) specific to the N terminus of moZP2 (37, 38). Confocal and DIC images of acrosome-intact and spontaneously acrosome-reacted sperm were obtained after incubation with donkey anti-rat immunoglobulin G (H + L) secondary antibody, Alexa Fluor 488 conjugate (1:100, Thermo Fisher), and Hoechst. The acrosome

status of human sperm was determined by immunostaining with antibodies to SPESP1 and CD46 to detect acrosome-intact and acrosome-reacted sperm, respectively (6).

Electron microscopy

Mouse sperm bound to beads were fixed in 2% glutaraldehyde in 0.1 M cacodylate buffer (pH 7.4) and incubated at 4°C for 2 hours. After extensive washing in the cacodylate buffer, beads were embedded in 2% agarose. The samples were then dehydrated through a graded series of ethanol and processed for embedding in LR White resin. Ultrathin sections were obtained with an ultramicrotome (Microm International GmbH) and mounted on formvar-coated nickel grids (Electron Microscopy Sciences). Ultrathin sections were counterstained with uranyl acetate followed by lead citrate and imaged in a Jeol JEM-1011 transmission electron microscope (Jeol).

Sperm-egg–binding assays

After treatment with hyaluronidase to remove cumulus cells, eggs were washed three times in HTF/BSA (9) and incubated with sperm freshly released from the epididymis (Acr^{EGFP}), sperm incubated for 1 hour in HTF/BSA medium ($Acr^{mCherry}$), or both types (1:1 ratio) of progressive motile sperm (final concentration, 1×10^5 ml^{-1}) suspended in 500 μl of HTF/BSA. After incubation (5 min), eggs were washed in HTF/BSA by careful transfer to a second and third dish. Fixed sperm and eggs were mounted in PBS with Hoechst (10 μg/ml) to identify nuclei. Bound sperm were quantified from Z projections obtained by confocal microscopy.

Mouse and human sperm binding to ZP2 peptide beads

IMAC Sepharose beads (100 μl; GE Healthcare Life Sciences) were incubated overnight (37°C, 90% N_2, 5% O_2, 5% CO_2) with recombinant moZP2$^{35–149}$ peptides in 100 μl of HTF/BSA and washed in the same medium to remove free peptide. The presence of the N terminus peptide on the agarose beads (37- to 100-mm diameter) was determined with a monoclonal antibody to the N terminus of ZP2 (6). Beads alone or moZP2 peptide beads were incubated (37°C, 90% N_2, 5% O_2, 5% CO_2) with freshly released Acr^{EGFP} (13) or 1 hour–incubated $Acr^{mCherry}$ mouse sperm in HTF/BSA (500 μl). Samples (20 to 50 beads) were collected at 5 min, 30 min, 60 min, 90 min, 3 hours, 4 hours, and 8 hours, fixed, washed and mounted in PBS with Hoechst. Bound sperm were quantified from Z projections, and acrosome status was determined by confocal microscopy. Concomitantly, the concentration and progressive motility of unbound sperm were evaluated at each time point. Alternatively, sperm were imaged live for 8 hours (37°C, 90% N_2, 5% O_2, 5% CO_2) while interacting with moZP2 peptide beads in HTF/BSA (500 ml) under mineral oil. A 60-μm Z series (5 μm each) was acquired at 15-s intervals to prevent sperm bleaching/damage.

Recombinant huZP2$^{39–154}$ peptides were attached to IMAC beads as described for moZP2 peptide. Beads alone or huZP2 peptide beads (6, 10) were incubated with freshly thawed or 2 hour–incubated human sperm in HTF/BSA (500 μl). Samples (20 to 50 beads) were collected over time and analyzed as described for mouse sperm binding.

Competitive sperm-binding assays

Eggs in cumulus from control (ICR) mice were incubated (37°C, 90% N_2, 5% O_2, 5% CO_2) with capacitated, progressive motile sperm (1×10^5 ml^{-1}) in the presence of beads alone or moZP2 peptide beads in HTF/BSA (500 µl). Sixteen hours later, eggs were collected, and fertilization was scored by the presence of two-cell embryos. Experiments were performed in triplicate. Alternatively, eggs in cumulus from hu*ZP2^Rescue* female mice were incubated (HTF/BSA, 500 µl; 37°C, 90% N_2, 5% O_2, 5% CO_2) with capacitated, progressive motile human sperm (1×10^5 ml^{-1}) in the presence of beads alone or huZP2 peptide beads. Sixteen hours later, eggs were fixed, stained with WGA-633 (Thermo Fisher) to visualize the zona pellucida, and mounted in PBS with Hoechst to quantify by confocal microscopy the number of supernumerary human sperm in the perivitelline space. Experiments were performed in triplicate.

Human sperm selection by peptide bead binding

Beads alone or coated with the huZP2$^{39–154}$ peptide were incubated (30 min, 37°C, 90% N_2, 5% O_2, 5% CO_2) with freshly thawed, progressive motile human sperm (1×10^5 ml^{-1}) in HTF (500 µl). Beads with sperm loosely attached were carefully transferred to a second dish containing HTF (50 µl). Sperm were released from beads by gentle pipetting and quantified by IVOS. In each sample, beads were removed by pipette under microscopic visualization, leaving the unbound sperm behind, and zona-intact immature human oocytes or ovulated eggs in cumulus from hu*ZP2^Rescue* female mice were added. As a control, a comparable number of sperm from the parental dish (before selection) were incubated (37°C, 90% N_2, 5% O_2, 5% CO_2) with hu*ZP2^Rescue* eggs in cumulus. Sixteen hours later, eggs were fixed, stained with WGA-633, and mounted in PBS with Hoechst (10 µg/ml). The number of sperm bound to the zona pellucida and present in the perivitelline space was quantified by Z projections using confocal microscopy. Experiments were performed using sperm from five different fertile donors.

In vivo ZP2 peptide bead contraception

Gonadotrophin-stimulated female mice were anesthetized with tribromoethanol (0.2 mg/10 g body weight). Beads alone, or moZP2 peptide beads (3×10^5), each diluted in 700 µl of HTF/BSA, were administered transcervically into both uterine horns using a syringe (1 ml) attached to a blunt plastic needle. To facilitate injections, anesthetized mice were positioned by grasping the tip of their tails to expose external genitalia. Care was taken to advance the needle no more than 1 cm beyond the cervix to ensure equal delivery into the two uterine horns. After recovery from the anesthesia, females were mated overnight with ICR males proven to be fertile. Those with a copulatory plug 24 hours after mating were euthanized to determine the number of one- and two-cell embryos within the oviduct. Alternatively, female mice administered with beads alone or moZP2 peptide beads (five in each experimental group) were co-caged with a medium (HTF)–treated female and mated with a male proven to be fertile.

To localize beads in the female reproductive tract, beads alone or moZP2$^{35–149}$ peptide beads were stained, respectively, with WGA-633 or IE-3 (1:50), a monoclonal antibody specific to the N terminus ofmoZP2 (37, 38). Stained beads were transferred transcervically,

and 1 hour later, females were anesthetized, perfused by cardiac puncture with PBS (60 ml) containing heparin (10 U/ml), and sacrificed. After isolation, the female reproductive tract was fixed overnight in 3% paraformaldehyde, washed three times in PBS, and clarified in ScaleA2 (20) for 4 weeks.

Ovulated eggs from $Cd9^{Null}$ mice fuse poorly with sperm, resulting in an accumulation of spermatozoa in the perivitelline space. To document interactions of sperm with moZP2 peptide beads in vivo and to determine whether sperm are able to penetrate the eggs' zonae pellucidae upon interaction with the ZP2 peptide beads in the uterus, $Zp3^{EGFP}$ female mice with green zonae pellucidae (23) in a $Cd9^{Null}$ background (24) were mated overnight with $Act^{mCherry}$; $Prm1^{EGFP}$; $Figla^{EGFP}$ male mice. Twenty-four hours after mating, females with copulatory plugs were anesthetized, perfused, and sacrificed as described. Their reproductive tracts were fixed and clarified before imaging with an Axioplan2 microscope equipped with an AxioCam ERc 5S camera (Carl Zeiss).

Statistics

All statistical analyses were performed with SigmaStat 12.3 (Systat Software). The original data are in table S2, and summaries of statistical analyses are in table S3. Descriptive statistics were used for human and mouse sperm binding, where the numbers of spermatozoa bound to zonae pellucidae or agarose beads were reported as box plots reflecting the median (horizontal line) and data points within the 10th and 90th percentiles (error bars) of three independent experiments. Boxes included the middle two quartiles, and outliers, when present, were indicated by dots. Three independent experiments were used to determine the number of eggs (avg ± SEM) with 0, 1, 2, 3, or >3 sperm in the perivitelline space for each experimental group. The total number of eggs analyzed was reported above each graph. The significance of differences in the avg ± SEM from three independent experiments evaluating in vitro and in vivo fertilization rates as well as CASAIVOS sperm parameters was determined using a one-way analysis of variance (ANOVA) followed by Tukey's test for multigroup comparison. The P value was considered statistically significant, and the number of biological replicates for all studies is included in the figure legends and table S3.

Supplementary Material

Refer to Web version on PubMed Central for supplementary material.

Acknowledgments:

REFERENCES AND NOTES

1. Gerland P, Raftery AE, Šev íková H, Li N, Gu D, Spoorenberg T, Alkema L, Fosdick BK, Chunn J, Lalic N, Bay G, Buettner T, Heilig GK, Wilmoth J, World population stabilization unlikely this century. Science 346, 234–237 (2014). [PubMed: 25301627]

2. Boivin J, Bunting L, Collins JA, Nygren KG, International estimates of infertility prevalence and treatment-seeking: Potential need and demand for infertility medical care. Hum. Reprod 22, 1506–1512 (2007). [PubMed: 17376819]

3. Lefièvre L, Conner SJ, Salpekar A, Olufowobi O, Ashton P, Pavlovic B, Lenton W, Afnan M,Brewis IA, Monk M, Hughes DC, Barratt CLR, Four zona pellucida glycoproteins are expressed in the human. Hum. Reprod 19, 1580–1586 (2004). [PubMed: 15142998]

4. Bleil JD, Wassarman PM, Structure and function of the zona pellucida: Identification and characterization of the proteins of the mouse oocyte's zona pellucida. Dev. Biol 76, 185–202 (1980). [PubMed: 7380091]

5. Bedford JM, Sperm/egg interaction: The specificity of human spermatozoa. Anat. Rec 188, 477–487 (1977). [PubMed: 409311]

6. Baibakov B, Boggs NA, Yauger B, Baibakov G, Dean J, Human sperm bind to the N-terminal domain of ZP2 in humanized zonae pellucidae in transgenic mice. J. Cell Biol 197, 897–905 (2012). [PubMed: 22734000]

7. Quesada V, Sánchez LM, Álvarez J, López-Otín C, Identification and characterization of human and mouse ovastacin: A novel metalloproteinase similar to hatching enzymes from arthropods, birds, amphibians, and fish. J. Biol. Chem 279, 26627–26634 (2004). [PubMed: 15087446]

8. Burkart AD, Xiong B, Baibakov B, Jiménez-Movilla M, Dean J, Ovastacin, a cortical granule protease, cleaves ZP2 in the zona pellucida to prevent polyspermy. J. Cell Biol 197, 37–44 (2012). [PubMed: 22472438]

9. Gahlay G, Gauthier L, Baibakov B, Epifano O, Dean J, Gamete recognition in mice depends on the cleavage status of an egg's zona pellucida protein. Science 329, 216–219 (2010). [PubMed: 20616279]

10. Avella MA, Baibakov B, Dean J, A single domain of the ZP2 zona pellucida protein mediates gamete recognition in mice and humans. J. Cell Biol 205, 801–809 (2014). [PubMed: 24934154]

11. Check JH, Adelson HG, Schubert BR, Bollendorf A, Evaluation of sperm morphology using Kruger's strict criteria. Arch. Androl 28, 15–17 (1992). [PubMed: 1550422]

12. Herbemont C, Sifer C, How to select the spermatozoon for intracytoplasmic sperm injection in 2015? Minerva Ginecol. 67, 185–193 (2015). [PubMed: 25581325]

13. Nakanishi T, Ikawa M, Yamada S, Parvinen M, Baba T, Nishimune Y, Okabe M, Real-time observation of acrosomal dispersal from mouse sperm using GFP as a marker protein. FEBS Lett. 449, 277–283 (1999). [PubMed: 10338148]

14. Hartmann JF, Gwatkin RBL, Hutchison CF, Early contact interactions between mammalian gametes in vitro: Evidence that the vitellus influences adherence between sperm and zona pellucida. Proc. Natl. Acad. Sci. U.S.A 69, 2767–2769 (1972). [PubMed: 4507601]

15. Chang MC, Fertilizing capacity of spermatozoa deposited into the fallopian tubes. Nature 168, 697–698 (1951).

16. Austin CR, Observations on the penetration of the sperm in the mammalian egg. Aust. J. Sci. Res. B 4, 581–596 (1951). [PubMed: 14895481]

17. Williams M, Hill CJ, Scudamore I, Dunphy B, Cooke ID, Barratt CLR, Sperm numbers and distribution within the human Fallopian tube around ovulation. Hum. Reprod 8, 2019–2026 (1993). [PubMed: 8150897]

18. Patrat C, Auer J, Fauque P, Leandri RL, Jouannet P, Serres C, Zona pellucida from fertilised human oocytes induces a voltage-dependent calcium influx and the acrosome reaction in spermatozoa, but cannot be penetrated by sperm. BMC Dev. Biol 6, 59 (2006). [PubMed: 17147816]

19. Bastiaan HS, Menkveld R, Oehninger S, Franken DR, Zona pellucida induced acrosome reaction, sperm morphology, and sperm–zona binding assessments among subfertile men. J. Assist. Reprod. Genet 19, 329–334 (2002). [PubMed: 12168733]

20. Hama H, Kurokawa H, Kawano H, Ando R, Shimogori T, Noda H, Fukami K, Sakaue-Sawano A,Miyawaki A, Scale: A chemical approach for fluorescence imaging and reconstruction of transparent mouse brain. Nat. Neurosci 14, 1481–1488 (2011). [PubMed: 21878933]

21. Haueter S, Kawasumi M, Asner I, Brykczynska U, Cinelli P, Moisyadi S, Bürki K, Peters AHFM,Pelczar P, Genetic vasectomy—Overexpression of Prm1-EGFP fusion protein in

elongating spermatids causes dominant male sterility in mice. Genesis 48, 151–160 (2010). [PubMed: 20095053]

22. Lin R-S, Jimenez-Movilla M, Dean J, Figla-Cre transgenic mice expressing myristoylated EGFP in germ cells provide a model for investigating perinatal oocyte dynamics. PLOS One 9, e84477 (2014). [PubMed: 24400092]

23. Zhao M, Gold L, Ginsberg AM, Liang L-F, Dean J, Conserved furin cleavage site not essential for secretion and integration of ZP3 into the extracellular egg coat of transgenic mice. Mol. Cell. Biol 22, 3111–3120 (2002). [PubMed: 11940668]

24. Le Naour F, Rubinstein E, Jasmin C, Prenant M, Boucheix C, Severely reduced female fertility in CD9-deficient mice. Science 287, 319–321 (2000). [PubMed: 10634790]

25. Jin M, Fujiwara E, Kakiuchi Y, Okabe M, Satouh Y, Baba SA, Chiba K, Hirohashi N, Most fertilizing mouse spermatozoa begin their acrosome reaction before contact with the zona pellucida during in vitro fertilization. Proc. Natl. Acad. Sci. U.S.A 108, 4892–4896 (2011). [PubMed: 21383182]

26. Cummins JM, Yanagimachi R, Sperm-egg ratios and the site of the acrosome reaction during in vivo fertilization in the hamster. Gamete Res. 5, 239–256 (1982).

27. Cates W Jr., Maggwa B, Family planning since ICPD—How far have we progressed? Contraception 90, S14–S21 (2014). [PubMed: 25033749]

28. Matzuk MM, McKeown MR, Filippakopoulos P, Li Q, Ma L, Agno JE, Lemieux ME,Picaud S, Yu RN, Qi J, Knapp S, Bradner JE, Small-molecule inhibition of BRDT for male contraception. Cell 150, 673–684 (2012). [PubMed: 22901802]

29. Amory JK, Muller CH, Shimshoni JA, Isoherranen N, Paik J, Moreb JS, Amory DW Sr.,Evanoff R, Goldstein AS, Griswold MD, Suppression of spermatogenesis by bisdichloroacetyldiamines is mediated by inhibition of testicular retinoic acid biosynthesis. J. Androl 32, 111–119 (2011). [PubMed: 20705791]

30. Li H, Ding X, Guan H, Xiong C, Inhibition of human sperm function and mouse fertilization in vitro by an antibody against cation channel of sperm 1: The contraceptive potential of its transmembrane domains and pore region. Fertil. Steril 92, 1141–1146 (2009). [PubMed: 18976756]

31. Su L, Mruk DD, Lie PPY, Silvestrini B, Cheng CY, A peptide derived from laminin-g3 reversibly impairs spermatogenesis in rats. Nat. Commun 3, 1185 (2012). [PubMed: 23149730]

32. Spargo SC, Hope RM, Evolution and nomenclature of the zona pellucida gene family. Biol. Reprod 68, 358–362 (2003). [PubMed: 12533396]

33. Palermo G, Joris H, Devroey P, Van Steirteghem AC, Pregnancies after intracytoplasmic injection of single spermatozoon into an oocyte. Lancet 340, 17–18 (1992). [PubMed: 1351601]

34. Bonduelle M, Camus M, De Vos A, Staessen C, Tournaye H, Van Assche E, Verheyen G,Devroey P, Liebaers I, Van Steirteghem A, Seven years of intracytoplasmic sperm injection and follow-up of 1987 subsequent children. Hum. Reprod 14 (Suppl. 1), 243–264 (1999). [PubMed: 10573038]

35. Rhim SH, Millar SE, Robey F, Luo AM, Lou YH, Yule T, Allen P, Dean J, Tung KS, Autoimmune disease of the ovary induced by a ZP3 peptide from the mouse zona pellucida. J. Clin. Invest 89, 28–35 (1992). [PubMed: 1370297]

36. Yauger B, Boggs NA, Dean J, Human ZP4 is not sufficient for taxon-specific sperm recognition of the zona pellucida in transgenic mice. Reproduction 141, 313–319 (2011). [PubMed: 21173071]

37. East IJ, Dean J, Monoclonal antibodies as probes of the distribution of ZP-2, the major sulfated glycoprotein of the murine zona pellucida. J. Cell Biol 98, 795–800 (1984). [PubMed: 6699085]

38. Sun W, Lou YH, Dean J, Tung KSK, A contraceptive peptide vaccine targeting sulfated glycoprotein ZP2 of the mouse zona pellucida. Biol. Reprod 60, 900–907 (1999). [PubMed: 10084964]
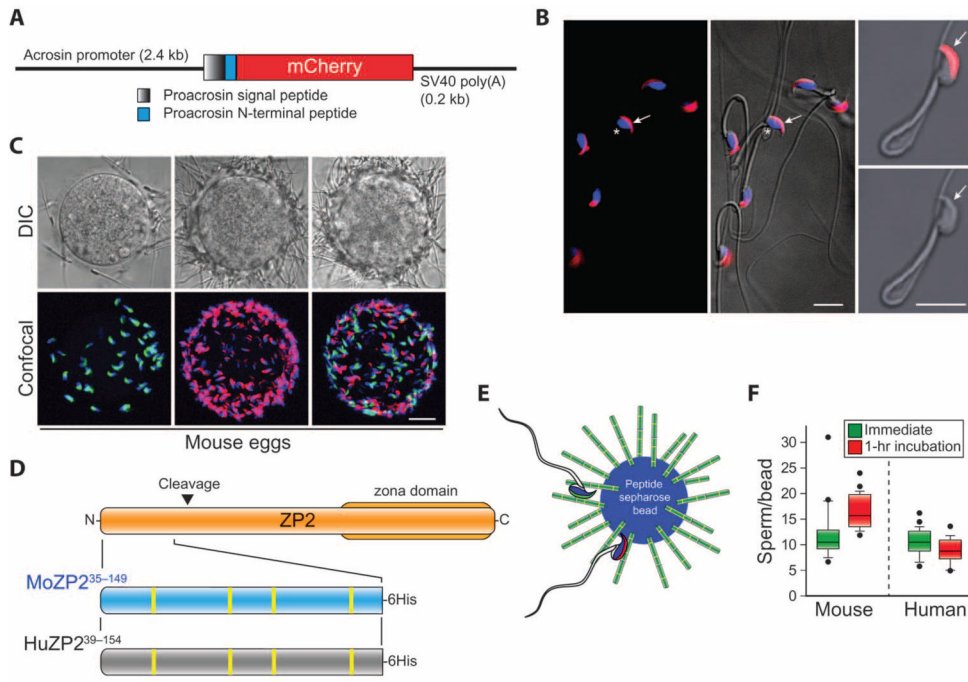
Fig. 1. Mouse and human sperm bind to the N terminus of ZP2.
(**A**) Schematic of the transgene used to establish the $Acr^{mCherry}$ transgenic mice. SV40 poly(A), SV40 simian virus polyadenylation signal. (**B**) Epididymal sperm isolated from $Acr^{mCherry}$ mice were fixed on polylysine-coated slides, stained with Hoechst, and imaged by confocal alone (left) or merged with differential interference contrast (DIC) microscopy (center). Two frames, 1.5-s apart, of a video before (top right) and after (bottom right) induction of acrosome exocytosis with calcium ionophore A23187. Arrows, acrosome; asterisk, nucleus. Scale bars, 10 μm. (**C**) Binding of sperm to cumulus-free mouse eggs using Acr^{EGFP} sperm freshly released from the epididymis (green, left) or $Acr^{mCherry}$ sperm after 1 hour of incubation in HTF/BSA (red, middle) alone or mixed (1:1) with the freshly released sperm (right). DIC (upper) and confocal Z projection (lower) images were obtained after fixation and staining with Hoechst (three biological replicates). Scale bar, 20 μm. (**D**) Schematic of moZP2$^{35–149}$ (blue) and huZP2$^{39–154}$ (gray) peptides at the N terminus of ZP2 (tan) that mediate sperm-egg binding in mice and humans, respectively. Inverted triangle, moZP2 postfertilization cleavage site (^{167}LA$^{↓}$DE^{170}); zona domain, ZP2$^{365–630}$; yellow vertical bars in lower flyout, cysteine residues. (**E**) Model of moZP2$^{35–149}$ or huZP2$^{39–154}$ peptide beads interacting with sperm freshly released from the epididymis (green) and incubated for 1 hour (red) in HTF/BSA before insemination. (**F**) Mouse sperm freshly released from the epididymis (left) and thawed human sperm (right) bound to moZP2$^{35–149}$ and huZP2$^{39–154}$ peptide beads, respectively, in comparable numbers when assayed immediately or after 1 hour (hr) of incubation in HTF/BSA before insemination. Neither human nor mouse sperm bound to beads alone control (three biological replicates) (fig. S1E). Box plots reflect the median (horizontal line) number of mouse or human sperm binding to peptide beads and data points within the 10th and 90th percentiles (error bars). Boxes include the middle two quartiles, and outliers are indicated by dots.
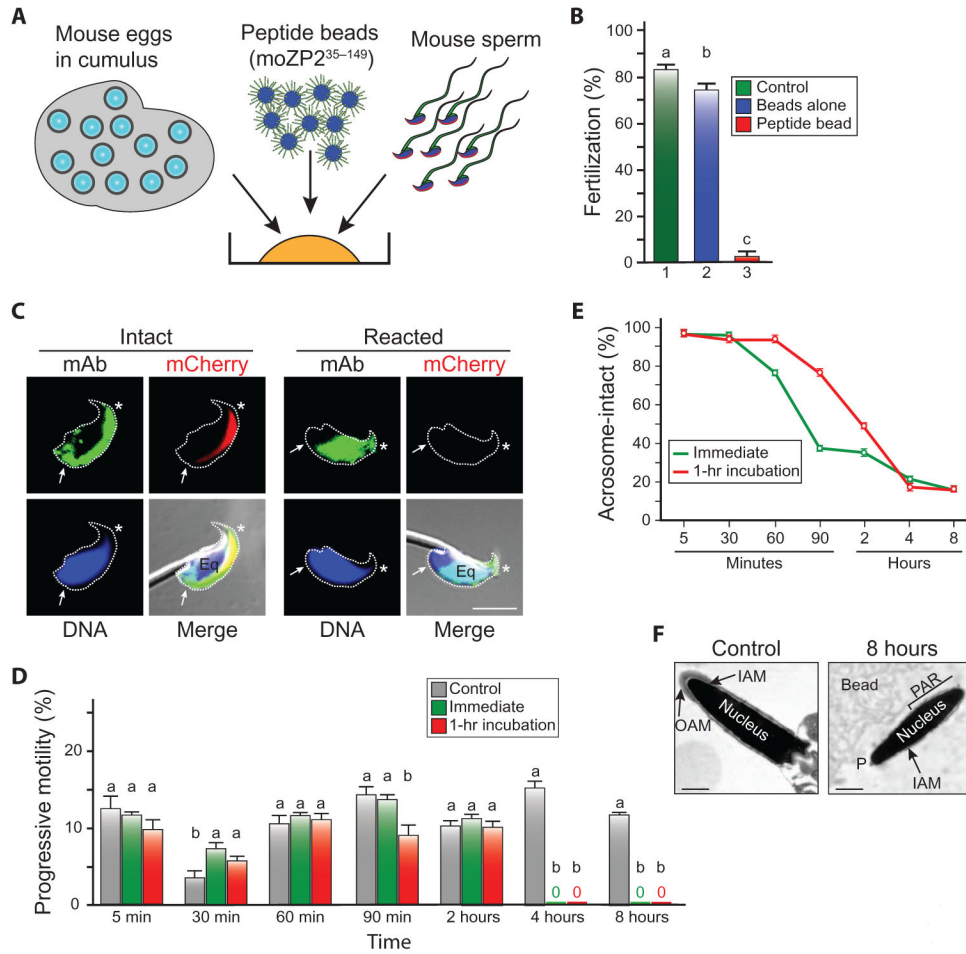
Fig. 2. The N terminus of moZP2 decoys sperm in vitro and prevents mouse fertilization.
(**A**) Schematic of in vitro fertilization, in which mouse eggs in cumulus mass were incubated overnight with 1×10^5 progressive motile mouse sperm in HTF/BSA (500 μl) alone, or in the presence of beads alone or moZP2$^{35-154}$ peptide beads (100 μl). (**B**) In vitro fertilization (%) after co-incubation of eggs in cumulus mass with medium (no beads) (1), beads alone (2), or ZP2 peptide beads (3) (three biological replicates). Statistical difference from control is indicated by a letter different than a; (b) $P = 0.027$; (c) $P < 0.001$. (**C**) Sperm from $Acr^{mCherry}$ (red acrosome) mice were incubated with moZP2$^{35-149}$ peptide before (left) or after (right) acrosome exocytosis, cross-linked with formaldehyde, immunostained with a monoclonal antibody (mAb) to the N-terminal ZP2 peptide (green), DNA-stained with Hoechst (blue), and imaged by confocal microscopy and DIC. Asterisk, acrosome; Eq, equatorial segment; arrows, postacrosomal region. Scale bar, 5 μm. (**D**) Progressive motility of unbound mouse sperm over 8 hours. Sperm were isolated either immediately after release from the epididymis or after 1 hour of incubation in HTF/BSA before incubation with ZP2 peptide beads. Control sperm were incubated with beads alone (three biological replicates). Statistical difference from control is indicated by a letter different than a (details in table S3). (**E**) Sperm were prepared as in (D), and the percentage of acrosome-intact sperm that remained bound to ZP2 peptide beads was determined over 8 hours (three biological replicates). (**F**) Electron microscopy of acrosome-intact (left panel) and acrosome-reacted
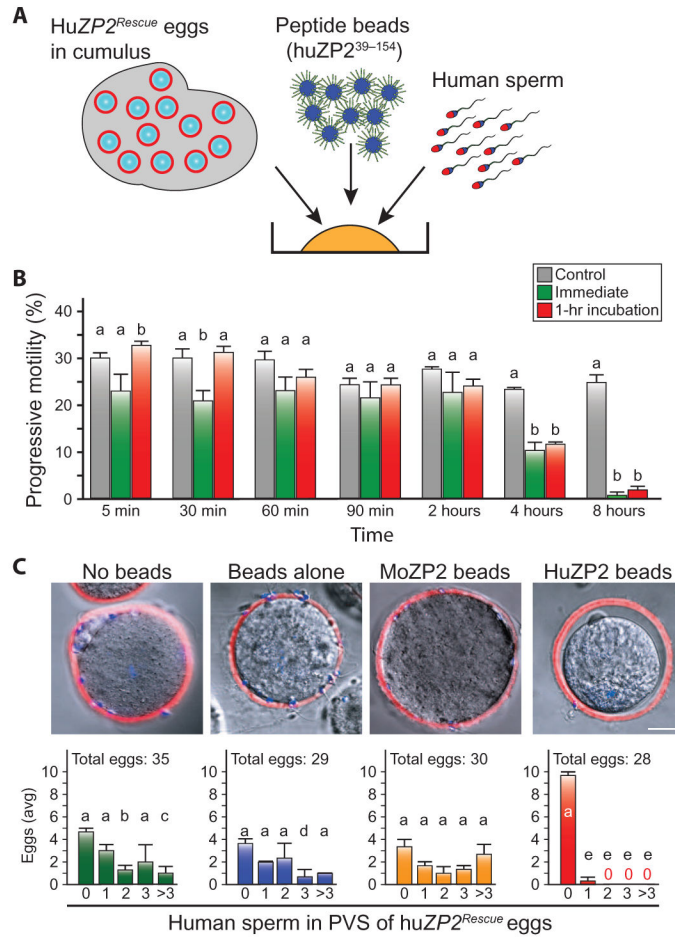
(right panel) sperm that remain bound to the ZP2 peptide beads 8 hours after insemination. IAM, inner acrosomal membrane. OAM, outer acrosomal membrane; PAR, postacrosomal region; P, perforatorium. Scale bar, 0.5 μm.

Fig. 3. The N terminus of huZP2 prevents zona matrix penetration of human sperm.
(A) Same as Fig. 2A except that 1×10^5 progressive motile human sperm were added to hu*ZP2*^{Rescue} eggs in cumulus with huZP2$^{39-154}$ peptide beads or beads alone. (**B**) Same as Fig. 2D except with human sperm (three biological replicates). Statistical difference from control is indicated by a letter different than a (details in table S3). (C) Hu*ZP2*^{Rescue} eggs in cumulus mass were inseminated with capacitated human sperm, in the presence of medium, beads alone, moZP2 peptide beads, or huZP2 peptide beads, and incubated overnight. Eggs were fixed and stained with wheat germ agglutinin, Alexa Fluor 633 conjugate (WGA-633) (red) and Hoechst (blue) to detect zonae pellucidae and nuclei, respectively. Scale bar, 10 μm. The numbers of eggs (avg ± SEM) with 0, 1, 2, 3, or >3 sperm in the perivitelline space (PVS) were determined for each experimental group (lower). Representative confocal and DIC-merged images of hu*ZP2*^{Rescue} eggs from each group are shown above the graphs. The total number of eggs analyzed in three independent biological replicates is indicated above each graph. Statistical differences from no sperm in the PVS is indicated by a letter different than a for each experimental condition: no beads, (b) $P = 0.040$ and (c) $P = 0.019$; beads alone, (d) $P = 0.026$; and huZP2 beads, (e) $P < 0.001$.
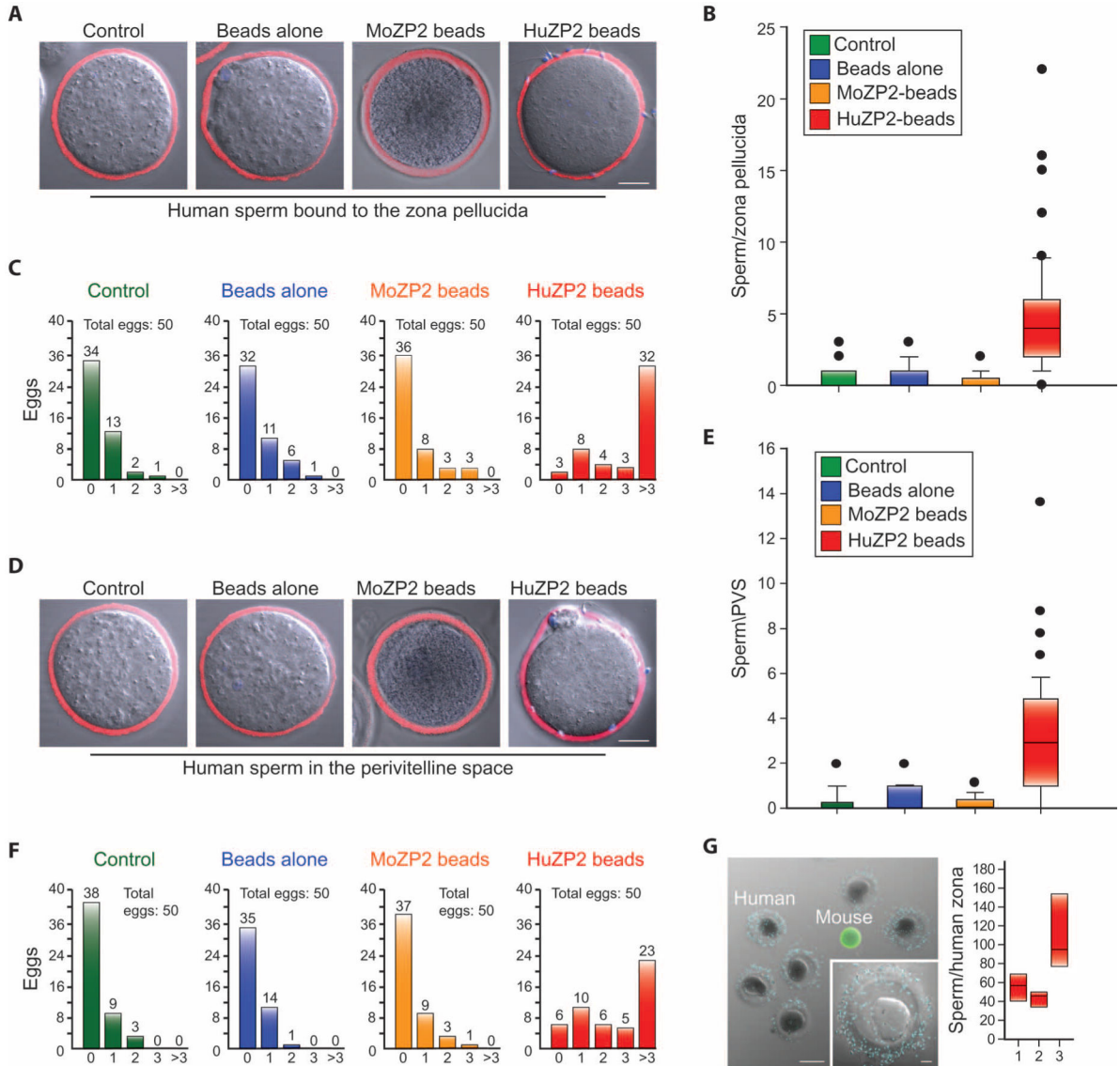
Fig. 4. Peptide beads select human sperm competent for binding and zona pellucida penetration.
(**A**) In the representative merged confocal and DIC images, human sperm (Hoechst-stained) from fertile donors were unselected (medium control or beads alone) or selected on the basis of short-term reversible binding to moZP2$^{35–149}$ or huZP2$^{39–154}$ peptide beads and tested for their ability to bind to the surface of the zona pellucida (stained with WGA-633) surrounding hu*ZP2*^{Rescue} eggs (see fig. S4, A and B, for individual donor data). Scale bar, 20 μm. (**B**) Box plots of sperm binding in (A) reflect the median (horizontal line) number of human sperm binding (cumulative data from five sperm donors) and data points within the 10th and 90th percentiles (error bars) (five biological replicates). Boxes include the middle two quartiles, and outliers are indicated by dots. (**C**) Human sperm were selected on the basis of short-term (30 min) reversible binding to ZP2 peptide beads (fig. S3C). The graphs show the number of hu*ZP2*^{Rescue} eggs with 0, 1, 2, 3, or >3 sperm bound to the zona surface after incubation with medium, beads alone, moZP2 peptide beads, or huZP2 peptide beads

using the sperm from five human donors. The total number of eggs analyzed in five biological replicates is indicated above each graph. (**D** to **F**) Same as (A) to (C) but assayed for sperm penetration into the perivitelline space (see fig. S4, C and D, for individual donor data). (**G**) Peptide bead selected human sperm (blue, Hoechst-stained nuclei) from fertile donors binding to zonae pellucidae surrounding premature human oocytes (left). $Zp3^{EGFP}$ mouse oocytes (green zona pellucida) served as a negative control. Scale bar, 100 μm; inset scale bar, 20 μm. The average number of selected human sperm (y axis) from three donors (x axis) binding to four or more zonae pellucidae (right) was analyzed as in (B).
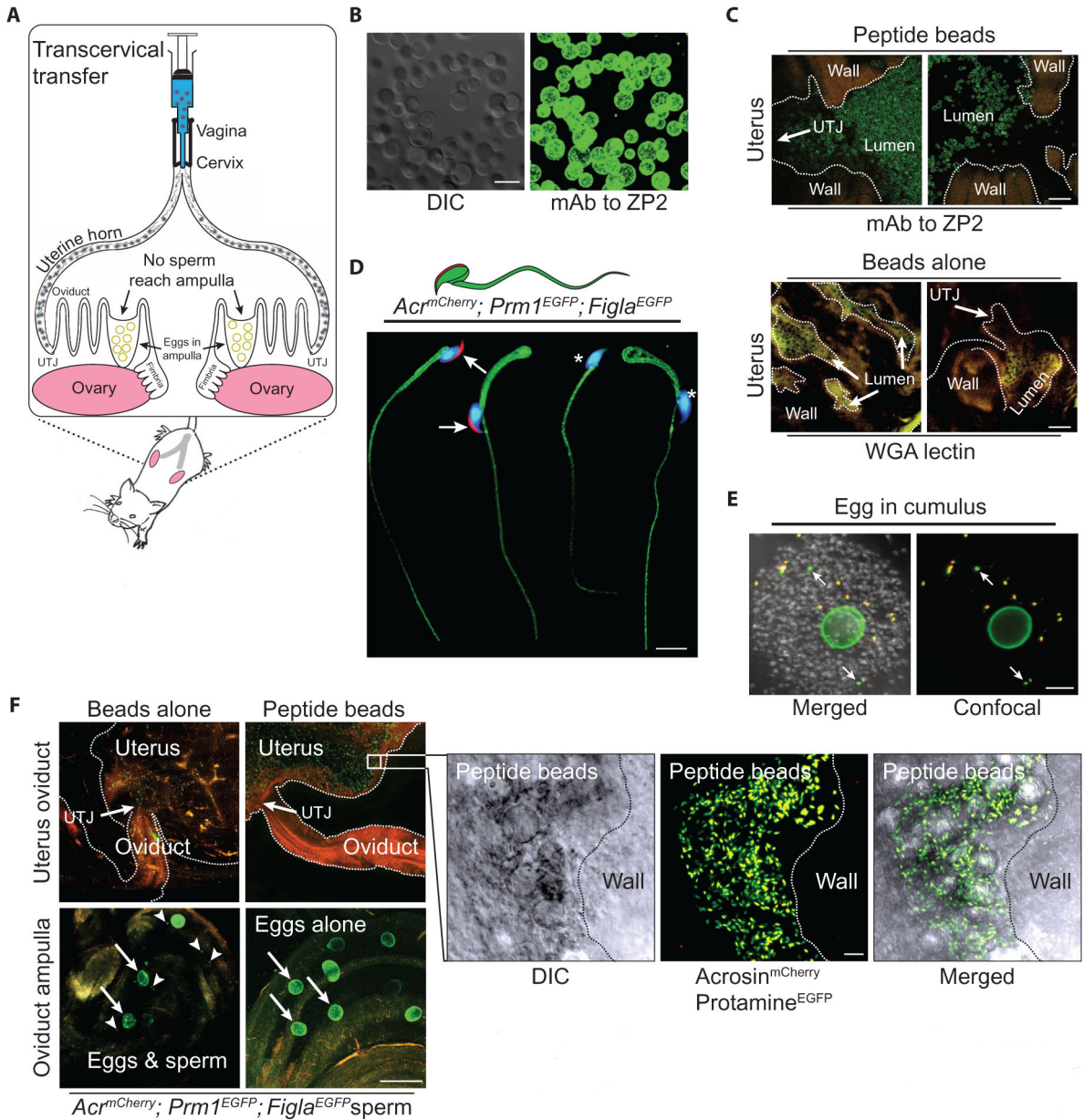
Fig. 5. MoZP2$^{35-149}$ acts as a sperm decoy in vivo.
(**A**) Schematic of female mouse reproductive tract with transcervical delivery of beads into the bilateral uterine horns. Interaction with moZP2 peptide beads in the uterus prevents normal sperm migration through the uterotubal junction (UTJ) into the oviduct, which results in female infertility. (**B**) MoZP2 peptide beads were stained with a monoclonal antibody to the N-terminal region of moZP2 and imaged by DIC (left) and confocal (right) microscopy. Scale bar, 50 μm. (**C**) MoZP2 peptide beads (top panel) and beads alone (bottom panel) were imaged in female uterine horns by confocal microscopy using monoclonal antibodies (green) to ZP2 and WGA-633 lectin (yellow), respectively, after cardiac perfusion and ScaleA2 clarification. Scale bars, 200 μm. (**D**) Spliced composite images of acrosome-intact (arrows) and acrosome-reacted (asterisks), Hoechst-stained

Acr^{mCherry}; *Prm1*^{EGFP}; *Figla*^{EGFP} sperm. Scale bar, 10 μm. (**E**) Insemination of *Zp3*^{EGFP} eggs in cumulus with *Acr*^{mCherry}; *Prm1*^{EGFP}; *Figla*^{EGFP} sperm. Mostly acrosome-intact (yellow) and fewer acrosome-reacted (green, arrows) sperm were visible through the cumulus mass after clarification. Scale bar, 50 μm. (**F**) *Zp3*^{EGFP}; *Cd9*^{Null} female mice were hormonally stimulated and mated with *Acr*^{mCherry}; *Prm1*^{EGFP}; *Figla*^{EGFP} male mice after transcervical administration of moZP2 peptide beads or beads alone (control) (three biological replicates). After clarification, confocal images (upper panels) were obtained to assay migration of fluorescently tagged sperm in the female reproductive tract. Outlines of organs (dotted lines) and the UTJ were apparent from background tissue autofluorescence. The flyout represents the higher magnification of sperm (green if acrosome-reacted; yellow if acrosome-intact) from the miduterine horn interacting with moZP2 peptide beads at single-cell resolution. In lower panels: arrows, eggs (green); arrowheads, sperm heads. Scale bar of panels, 200 μm; scale bar of the flyout, 20 μm.
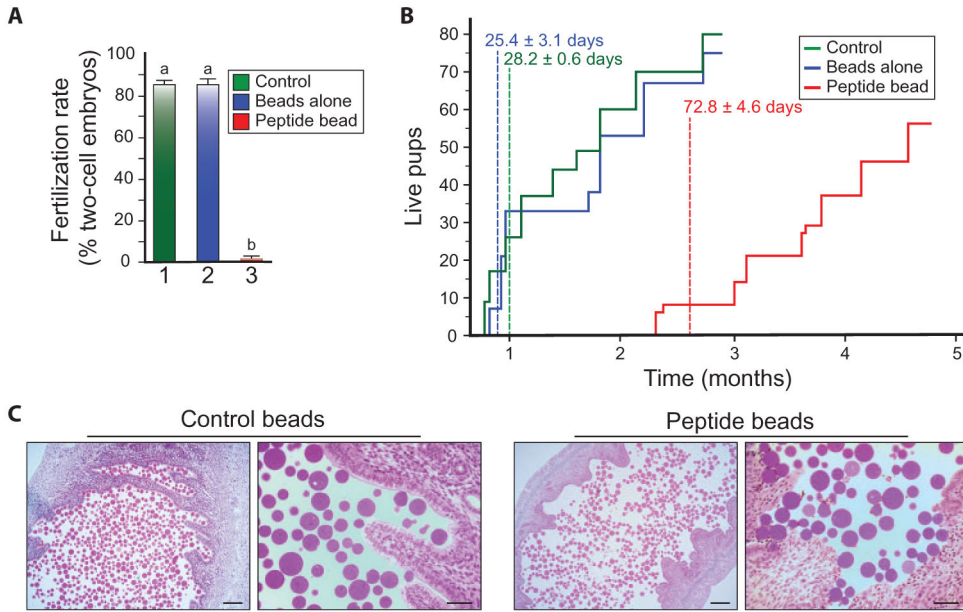
Fig. 6. MoZP2$^{35-149}$ peptide beads provide long-term, reversible contraception.
(**A**) Female mice were mated after transcervical administration of medium (control), beads alone, or moZP2 peptide beads, and fertilization was determined 40 hours later by the presence of two-cell embryos (as a percentage of total two-cell embryos plus unfertilized eggs in the oviduct; three biological replicates). Statistical difference from control is indicated by a letter different than a ($P < 0.001$). (**B**) The number and time of live births from two litters each of five female mice continuously mated after transcervical administration of medium (control), beads alone, or moZP2 peptide beads. The numbers shown on the graph indicate the time of the first pups' birth, expressed as the number of days (avg ± SEM) after the start of mating. (**C**) Light microscopic images of female reproductive tract 2 weeks after treatment with beads alone or moZP2 peptide beads. Left panels: scale bars, 150 μm; right panels: scale bars, 50 μm.